MOLECULAR DYNAMICS SIMULATION OF THE PRIMARY PROCESSES IN THE PHOTOSYNTHETIC REACTION CENTER OF *RHODOPSEUDOMONAS VIRIDIS*

H. TREUTLEIN *, C. NIEDERMEIER *, K. SCHULTEN *,
J. DEISENHOFER +, H. MICHEL +,
A. BRÜNGER † ‡, M. KARPLUS †

* *Physik-Department, Technische Universität München, D-8046 Garching, FRG*

\+ *Max-Planck-Institut für Biochemie, D-8033 Martinsried, FRG*

† *Department of Chemistry, Harvard University, Cambridge, MA 02138, USA*

‡ *Yale University, New Haven, CT 06511*

ABSTRACT. We have carried out a computer simulation of the photosynthetic reaction center of *Rhodopseudomonas viridis* based on the available molecular structure[1,2]. Our simulation employed the CHARMM program[3] in conjunction with the socalled stochastic boundary method[4,5]. Electron transfer has been modeled by re-charging the respective chromophores assuming charge distributions based on quantumchemical (MNDO) calculations. Our results suggest, that the high efficiency of the initial charge separtation is achieved (i) by a highly optimised geometry of chromophores for forward electron transfer and (ii) by hindering the electron back transfer via motions of protein constituents.

1. Introduction

The photosynthetic reaction center is a large protein located in the cell membran of the bacterium *Rhodopseudomonas viridis*[1,2]. Inside of this protein there are four heme groups (in a cytochrome subunit), 4 bacteriochlorophylls b, two bacteriopheophytins, one menaquinone, one ubiquinone and carotenoid. The protein absorbs light by a bacteriochlorophyll dimer called *special pair*. The light energy

A. Pullman et al. (eds.), Transport Through Membranes: Carriers, Channels and Pumps, 513–525.

is then converted into an electron gradient across the membrane by transferring electrons (and holes) inside the protein along the chromophores. One main open question regarding the photosynthetic reaction center concerns the high efficency with which an electron and a hole are separated by light absorbtion in the system and their recombination is being prevented.

In our work we have investigated control of electron transfer rates through the electrostatic field inside the protein and through mechanical motion of the chromophores and their surrounding protein matrix which can either establish or hinder electrical contact. Since the time scale of the process under consideration is close to the time scale accessible to computer simulations of protein dynamics, the reaction center is an excellent candidate for a molecular dynamics study.

2. Method

The calculations we describe in this article were based on the X-ray structure of the reaction center of *Rhodopseudomonas viridis* at 3 Å resolution[1,2]. All charge distributions of the neutral and ionized chromophores have been calculated by means of the all valence electron MOPAC quantum chemistry program[6]. The molecular dynamics calculations involved the CHARMM program in connection with the method of stochastic boundaries[4,5], which allowed us to select a central part of the reaction center for the simulation. The selected part contained 3634 atoms inside a sphere of 25Å, which includes all chromophores except three heme units of the cytochrome.

Fig. 1 displays the chromophore structure inside the simulated protein segment (reaction and buffer region) together with their abreviated names. Light is absorbed by the *special pair*. Then an electron is transferred from the *special pair* to the bacteriopheophytine BPL, from there to the menaquinone QA and then via an iron ion FE1 to a ubiqinone QB. This ubiquinone and also the carotenoid are not included in our segment and and therefore not shown in Fig. 1, because they both were not seen in the 3Å resolution X-ray data, our calculations were based on. Phytol chains of the non-functional branch chromophores (BCMP, which is part of the *special pair* dimer, BCMA and BPM) are partially located inside the buffer region, which implies that some of their atoms are constrained to their initial positions. This induces dynamical artifacts, that must be considered when trying to compare the dynamical properties between the functional (BCLP, the other cromophore of the *special pair*, BCLA, BPL, QA and the iron-ion FE1) and the non-functional chromophores. (Of the functional chromophores only a few atoms of the quinone QA lie inside the buffer region.

The following molecular dynamics calculations were carried out:

— After minimizing the atomic coordinates provided by Deisenhofer and Michel according to CHARMM's energy function, we started a 20*ps* simulation

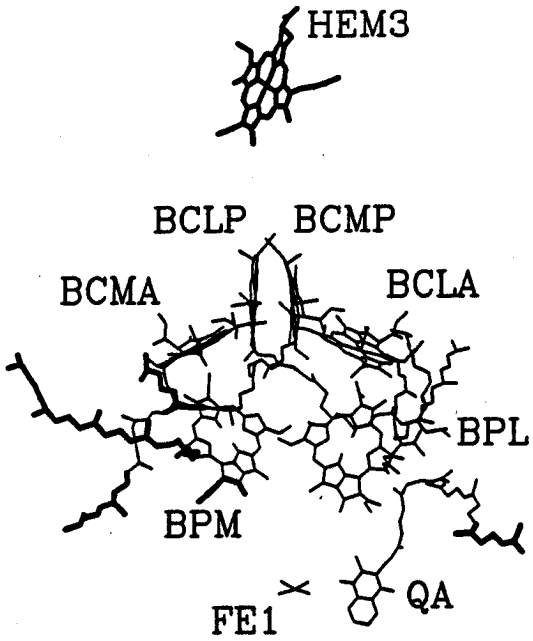

Fig. 1. Structure of chromophores in the simulated protein-segment together with their abbreviated names. Bonds between atoms inside the buffer region are denoted by thick solid lines.

with randomly chosen velocities according to a *Maxwell*-distribution at 300 K. This procedure allowed the reaction center segment to equilibrate for 20 ps to a state with relaxed sterical interactions.

— The second run, in the following referred to as run A, simulated for 20 ps the dynamics of the reaction center before the primary electron transfer. Therefore the charge states of the *special pair* and the bacteriopheophytin have been chosen to be neutral. The motion resulting from run A had been analyzed.

— We then transferred an electron charge from the *special pair* to the bacteriopheophytin (BPL) by removing one electron from the highest occupied orbital of the *special pair* bacteriochlorophyll distant from the functional branch and depositing this electron into the lowest unoccupied orbital of the functional bacteriopheopytin.

— We then carried out a third simulation, in the following referred to as run B, which monitored the dynamics of the reaction center, thus perturbed, for

20 ps. The resulting motion was analyzed and compared with the behaviour before the electron transfer.

— We also simulated an iron-depleted reaction center for 20 ps. We removed the iron-ion FE1 from our segment and investigated the resulting structural modifications. Details of this calculation are described in[7]

We have also studied the mean electrostatic potential on the chromophores[8]. For this purpose we included Coulomb interactions with fractional charges on all reaction center atoms including hydrogens. The mean electrostatic potentials of the individual chromophores were obtained in two steps:

1. A negative test charge $(-e)$ was brough from infinity (∞) to the central chromophore (tetrapyrol rings and quinone, menaquinone rings) atoms at positions $\vec{r}$ and the energy difference $\Delta V(\vec{r}) = V(\vec{r}) - V(\infty)$ was determined by summing the Coulomb contributions of all charges inside the reaction center, with the exception of the charges on the same tetrapyrol or quinone rings. The influence of the latter should be attributed to the redox energy of a chromophore. In case of the special pair (SP) the Coulomb interactions between the two tetrapyrol moieties were also not counted.
2. The mean potential was then evaluated by averaging over the potential differences $\Delta V(\vec{r})$ of all atoms belonging to the ring systems of the individual chromophores.

These calculations are obviously a first approximtion of the true reaction center electrostatics, since we have not included any water or membrane region outside and dielectric screening inside the protein.

3. Results and discussion

3.1. MEAN ELECTROSTATIC POTENTIAL

One important result of our investigation of the electrostatics inside the reaction center can be explained in Fig. 2. There the mean electrostatic potential levels of all chromophores are shown. The *special pair* has been positively charged to describe the transfer processes. The heme energy levels are found to be more positive than those for the other chromophores in accordance with the function of the hemes as hole carriers. However, the heme energies are spread over a very broad energy range. We attribute this to a neglect of the water fraction surrounding the cytochrome unit and contributing an effective dielectric screening. The energy levels of the M (non-functional) branch chromophores QB, BCMA, BPM are more negative than their L (functional) branch counterparts. This is opposite to the findings of Yeates et

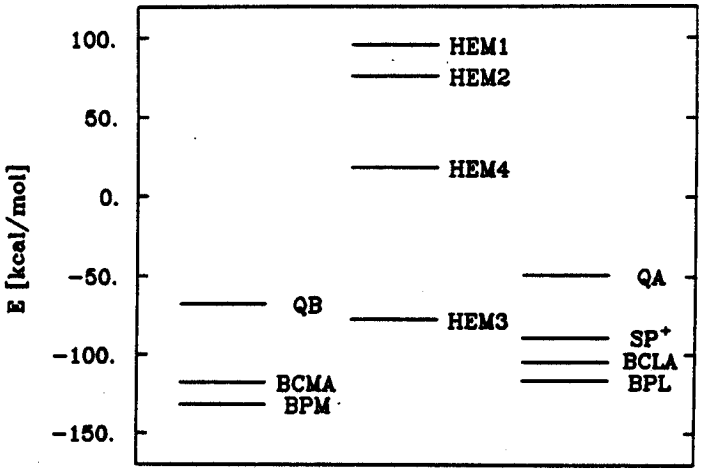

Fig. 2. Mean electrostatic potential levels of reaction center chromophores. The calculations are based on the X-ray structure.

al.[9] for the *Rps. sphaeroides* reaction center which also accounted for the effect of a heterogeneous dielectric (water–membrane) surrounding. The quinone energy levels lie above all the chlorophyll and pheophytine energy levels. We attribute this to Coulomb repulsion with the net six negative charges on the H-unit of the photosynthetic reaction center. A neutralization of the six negative surface charges of the H-unit through H^+ is likely to lower considerably the quinone energy levels[8]. In this respect it is interesting to note that the H-unit channels protons to the QB binding site, i.e. it is functionally favourable to have a high local concentration of protons near the H-unit.

The remaining ordering of energy levels of the functional branch chromophores BCLA and BPL is in accordance with the known features of primary electron transfer. The accessory chlorophyl (BCLA) energy level lies considerably above the pheophytine energy level. Considering the redox energy difference[10] $E_m(Chl) - E_m(Ph) \approx 5\frac{kcal}{mol}$ in identical solvents (Chlorophyll is more difficult to reduce than Pheophytine) the actual energy level of a reduced accessory Chlorophyll BCLA is not available for thermally assisted light-induced electron transfer.

3.2. THERMAL MOTION

Thermal motion of the protein atoms induces fluctuations of the atomic positions $\vec{r}_j$ around their equilibrium values $< \vec{r}_j >$. The simpliest measure of these fluctuations

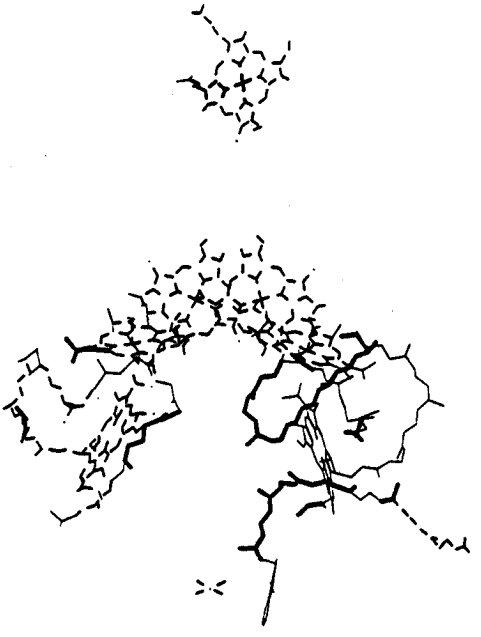

Fig. 3. Flexibility of chromophore atoms during run A. Dashed bonds are drawn between atoms whose root mean square deviations of the mean atomic position σ is less than 0.4 Å, very flexible atoms ($\sigma > 0.7$ Å) are connected by thick lines.

is given by the root mean square deviations $\sigma_j = \sqrt{< (\vec{r}_j - < \vec{r}_j >)^2 >}$. σ_j, which can differ for different locations in the protein, provides a measure of the local flexibility of a protein.

The root mean square deviations of the chromophores during run A are illustrated in Fig. 3 : Dashed bonds are drawn between atoms that exhibit only a small degree of flexibility during run A, thick bonds denote atoms exhibiting a high degree of flexibility. The special pair ring structure turns out to be the most rigid part of the chromophore branches ($\sigma < 0.3$ Å). This rigidity might be important for the function of the *special pair* . The pheophytin ring and the phytol chains are found to be most flexible. The pheophytine BPL appears to be located in a small "pocket" inside the protein, which accounts for its mobility. The high flexibility can contribute to the different rates of forward- and backward electron transfer by allowing BPL to be shifted after primary electron transfer into a position unfavourable for the back-transfer.

3.3. CORRELATED FLUCTUATIONS

In addition to the mobility of each chromophore it is important to get information about the correlated motion of chromophores among one another. Therefore we calculated the covariance C_{ik} between fluctuations of pairs of atoms i and k from all chromophores. This quantity is defined as

$$C_{ik} = \frac{c_{ik}}{\sqrt{c_{ii}c_{kk}}}$$

$$c_{ik} = < (\vec{r}_i - < \vec{r}_i >) \cdot (\vec{r}_k - < \vec{r}_k >) > \ .$$

Values of the covariance near +1 or −1 indicate that atomic motions are tightly coupled in phase (+1) or out of phase (−1), values around zero indicate a loose coupling. C_{ik} can differentiate between domains of the protein for which thermal fluctuations do not alter very much interatomic (inter-chromophore) distances ($C_{ik} \approx 1$) from domains where thermal fluctuations lead to strong variations of these distances ($C_{ik} \approx 0$). We found, that strong (positive) correlations, i.e. ≥ 0.3, among different chromophores occur within a range of 10Å.

To illustrate our findings Fig. 4 provides results on the covariances between the bacteriopheophytine BPL and one *special pair* bacteriochlorophyll BCLP. The Figure shows that the motion of the phytol chain of one of the BCLP is strongly coupled in phase to the pheophytine ring. This dynamic coupling, essentially an intermolecular attraction, could provide the interaction needed for the photo-induced primary electron transfer between the special pair and BPL in case the transfer involves the BCLP phytol chain. This attraction would prevent any thermal motion from impeding the fast (3 ps) primary electron transfer.

We have also investigated the covariance between motions of the remaining chromophores. The chromophores consecutive along the electron transfer route BCMP, (BCLA ?), BPL, QA are coupled pairwise in phase, i.e. BCMP to BCLA, BCLA to BPL .... Also both *special pair* chlorophyll-ring systems are strongly coupled, building a sandwich complex. This implies that thermal fluctuations do not affect very much the relative distances between these chromophores. This could indicate that the chromophore arrangement is optimized for the electron (forward) transfer and that structural disturbances due to the inherent thermal mobility are kept at a minimum. This feature obviously can have important implications for the mechanism of primary ellectron transfer: edge to edge couplings between the chromophores, which without this feature may be unreliable due to thermal motions, might have been tuned to rather precise values in the reaction center to provide a most effective forward electron transfer. This idea is also supported by the results

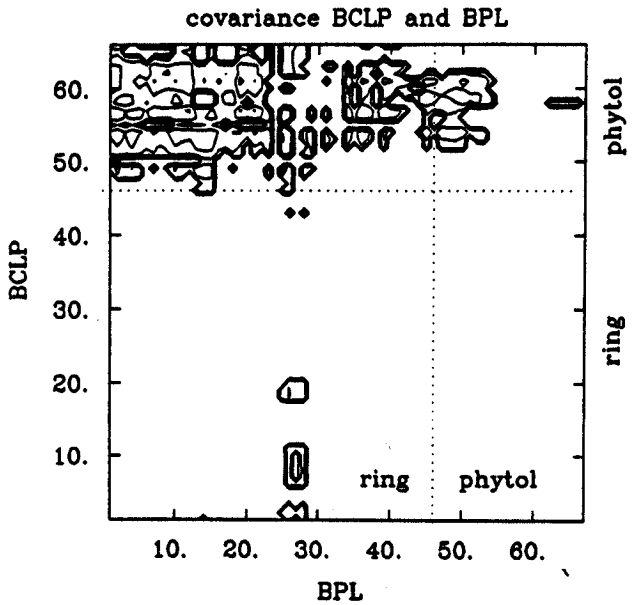

Fig. 4. Covariances C_{ik} between the atoms of BCLP and BPL.) The axes present the atomic labels i and k. All correlations C_{ik} are positive. The blank area denotes pairs of atoms i, k with correlations smaller than 0.3. *Contour lines which separate regions with larger correlations are shown; the contour lines correspond to increments of* 0.1.

of a simulation of an iron-depleted reaction center (this means that the FE1 iron ion of Fig. 1 has been removed) we have performed[7] and compared with experimental results of Kirmaier and Debus[11,12].

3.4. RESPONSE TO ELECTRON TRANSFER

Our simulations (run A and B) show, that a sudden jump of the electron from the *special pair* to the functional bacteriopheophytin disturbs the protein structure.

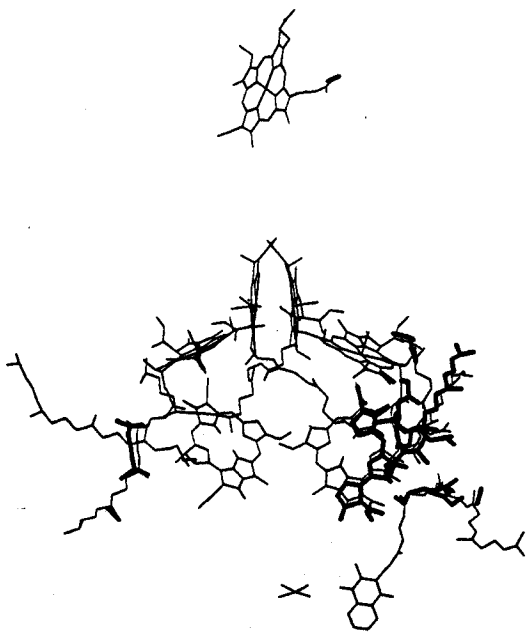

Fig. 5. Structural differences induced by primary electron transfer. The average structure of run B is represented by thin lines. The average structure of run A is overlayed by thick lines for those atoms the positions of which differ between the two structures by more than 0.4 Å.

In Fig. 5 we present the average structure of run B. The mean structural difference to the average structure of run A is found to be 0.32 Å. For atoms whose position has changed by more than 0.4 Å the average structure of run A is also displayed in Fig. 5. The largest structural differences occur for the pheophytine BPL and the (phytol) chains. After the electron is transferred, BPL is shifted towards the *special pair* . This motion is induced by the additional Coulomb interaction between the (after the electron transfer) positively charged special pair and the negatively charged pheophytine. This might hinder the backtransfer of the electron

by altering the alignment of the chromophores BCMP, BCLA, BPL or the tight interaction of BPL with the BCLP phytol chain. It is also possible that the cleft-like pocket mentioned above inside the L subunit furnishes some degree of control during the primary electron transfer by altering the chromophore – chromophore interactions through the resulting mobility and also allowing for fast and effective dielectric relaxation (see also Ref. 8). In order to to discuss this issue in the light of Marcus' theory of electron transfer[13] we investigated the electrostatic energy differences due to electron transfer.

3.5. FLUCTUATING AND TIME-VARYING ELECTROSTATIC ENERGY

Because of the weak coupling between covalent and ionic states , i.e. SP^*–BPL and SP^+–BPL^-, compared with vibrational energies in the system, electron transfer is possible only when covalent and ionic states are accidentally degenerate. This corresponds in the theory of Marcus[13] to a transition between covalent and ionic states only at crossings of potential energy surfaces. Due to Coulomb interactions with the surrounding protein matrix the energy difference between the covalent and ionic states fluctuates in accordance with thermal motions of the protein. The energy difference can also vary in time when the protein undergoes structural transitions, e.g. those induced by electron transfer between the chromophores. Obviously, the protein can regulate then through its motion the rate of electron transfer by controlling the coincidences of energy values of covalent and ionic states. We have investigated, therefore, how this energy difference for the primary electron transfer $\Delta E = E(SP^+\text{–}BPL^-) - E(SP^*\text{–}BPL)$ varies during the simulated motion of a protein both before and after electron transfer. It should be pointed out, that electron transfer is controlled also by internal degrees of freedom, which can also be described by Marcus theory or by its quantum-mechanical generalizations.

In order to interprete the results of a molecular dynamics simulation regarding the energy $\Delta E(t)$ it is important to realize that **CHARMM** can only account for contributions to $\Delta E(t)$ due to interactions with charges outside the range of atoms which carry the positive and negative charge in the respective chromophores: Included in such calculations are neither the redox energy difference[10] which roughly measures $20\frac{kcal}{mol}$ for the SP^*– BPL $\rightarrow$ SP^+-BPL^-– transfer, nor the Born energy relative to the polar solvents, e.g. DMF, in which redox energies are measured. Assuming a dielectric constant of $\epsilon \approx 2$ inside the protein, the Born energy for moving a single charge from DMF to the protein $\Delta E_B = \frac{e^2}{2r}(\epsilon^{-1} - \epsilon_{DMF}^{-1})$ for $r \approx 5\mathring{A}$ measures about $10\frac{kcal}{mol}$, twice that for two charges, and, hence, a total energy of about $40\frac{kcal}{mol}$ needs to be added to the pure external electrostatic contribution. This is, of course, a very rough estimate.

Uncertainties in the redox and Born energies don't allow to determine zero cross-

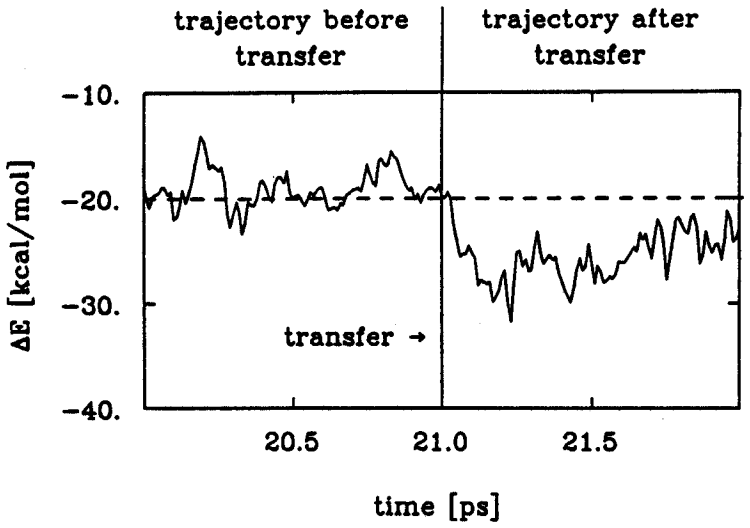

Fig. 6. Energy difference ΔE before and after electron transfer from special pair to BPL. The left part of the diagram displays ΔE obtained from molecular dynamics data (trajectory) before transfer. The instant the electron is transferred by changing the charge distribution on the special pair and BPL is denoted by an arrow. The right part shows ΔE after transfer obtained from molecular dynamics data (trajectory) after transfer.

ings of the energy difference between covalent and ionic states in proteins and, for that reason, we will present in Fig. 6 only the electrostatic fraction of this energy difference. The electrostatic energy difference presented there has been calculated using CHARMM's electrostatic energy function described above. We calculated these energy-differences both for a simulation before electron transfer and after the ransfer.

The result for the electrostatic energy difference $\Delta E(t)$ describing a transfer from the *special pair* to the pheophytine BPL is presented in Fig. 6. The left part of the diagram shows ΔE before the transfer: it fluctuates around an energy value of about $-20\frac{kcal}{mol}$. On the basis of a value of $40\frac{kcal}{mol}$ for the further contributions to the SP^*–BPL and SP^+–BPL^- energy difference one estimates an approximate energy of $-20 + 40 = 20\frac{kcal}{mol}$ for the excitation energy of the special pair.

It is suggestive to regard the crossings with the mean value $-20\frac{kcal}{mol}$ as the occurrences of energy degeneracies between the SP^*–BPL and SP^+–BPL^- energy levels. If this analogy holds , primary electron transfer is possible any time a

crossing occurs. This behaviour demonstrates that protein fluctuations can control primary electron transfer.

We want to consider now how electron transfer affects $\Delta E(t)$ and, in particular, if back-transfer can be controlled (hindered) by protein relaxation and fluctuation. We have transferred, therefore, an electron in our simulations (by altering the chromophore charge distributions) at the instant marked by an arrow in Fig. 6 (at the time labeled 21 ps). $\Delta E(t)$ within 0.3 ps after the transfer decreases by about $10\frac{kcal}{mol}$ and then relaxes to a value close to $-25\frac{kcal}{mol}$. This is $5\frac{kcal}{mol}$ below the $-20\frac{kcal}{mol}$ value before transfer which at room temperature is just enough to prevent further crossings with the $-20\frac{kcal}{mol}$ line and, hence, back-transfer. It might be interesting to note that the very rapid initial relaxation appears to be very effective in preventing back-transfer already after about 100 fs. Furthermore, relaxations are sufficient to prevent back-transfer, however, do so with a minimal (exothermic) energy loss.

4. Acknowledgements

The authors like to thank Z. Schulten, P. Tavan and W. Nadler for advice and help. This work has been supported by the Deutsche Forschungsgemeinschaft (SFB 143-C1) and by the National Center of Supercomputer Applications in Urbana, IL.

References

1. J. Deisenhofer, O. Epp, K. Miki, R. Huber, H. Michel, *J Molec Biol* 180, 385 (1984)
2. J. Deisenhofer, O. Epp, K. Miki, R. Huber, H. Michel, *Nature* 318, 618 (1985)
3. B. R. Brooks et al. , *J Comp Chem* 4, 187 (1983)
4. C. L. Brooks, A. Brünger, M. Karplus, *Biopolymers* 24, 843 (1985)
5. A. Brünger, R. Huber, M. Karplus, *Biochem* 26, 5153 (1987)
6. M. J. S. Dewar and W. Thiel, *J. Am. Chem. Soc.* 99 (1977) 4899
7. H. Treutlein, *et al.*, in *The photosynthetic bacterial reaction center: Structure and dynamics*, J. Breton, A. Vermeglio, Ed. (Plenum Press, London 1988) p.139-150
8. H. Treutlein, *et al.*, in *The photosynthetic bacterial reaction center: Structure and dynamics*, J. Breton, A. Vermeglio, Ed. (Plenum Press, London 1988), p.369-377

9. T. O. Yeates et al., *PNAS* 84, 6438 (1987)
10. Fajer et al., *JACS* 100,1918 (1978)
11. C. Kirmaier et al., *PNAS* 83, 6407 (1986)
12. R. J. Debus, G. Feher, M. Y. Okamura, *Biochemistry* 25, 2276 (1986)
13. R. A. Marcus, N. Sutin, *Biochim Biophys Acta* 811, 265 (1985)